Absolute separation energies for Na clusters

J. Borggreen,[1] K. Hansen,[1,2] F. Chandezon,[1,3] T. Døssing,[1] M. Elhajal,[1,4] and O. Echt[1,5]
[1]*University of Copenhagen, Niels Bohr Institute, 2100 Copenhagen, Denmark*
[2]*Institute of Physics and Astronomy, University of Aarhus, Ny Munkegade, 8000 Aarhus C, Denmark*
[3]*Département de Recherche Fondamentale sur la Matiére Condensée, SI2A, CEA Grenoble, 17, Rue des Martyrs, 38054 Grenoble Cedex 9, France*
[4]*Laboratoire Louis Neel, 25, Avenue des Martyrs, 38042 Grenoble Cedex 9, France*
[5]*Physics Department, University of New Hampshire, Durham, New Hampshire 03824*
(Received 28 December 1999; published 8 June 2000)

Na clusters in the size range of 50–400 atoms are led to evaporate in a heat bath with controlled temperature. For cluster sizes around closed shells, decay rates are determined as a function of temperature. For temperatures below 357 K they all agree with an Arrhenius law and allow absolute separation energies to be extracted. Separation energies are presented and compared to previously determined (relative) values. Enhanced shell effects are observed in the heat bath experiments. Deviations from the Arrhenius law at intermediate temperatures are discussed.

PACS number(s): 36.40.Qv, 61.46.+w, 36.40.Cg

I. INTRODUCTION

The electronic shell structure of simple metal clusters was originally revealed in measurements of abundance spectra of initially hot clusters evaporating in vacuum [1]. This type of experiment has been dominating so far, but a quantitative description of the evaporation is complicated by the fact that each individual cluster adopts its own temperature during the process [2]. Successful efforts have been made to extract (relative) cluster separation energies in a quantitative manner [3,4]. However, the shell effect is relatively weak in the spectra and quickly diminishes as cluster sizes increase. It has been a wish to be able to control the cluster temperature during evaporation, for two reasons: firstly, by knowing the temperature one obtains an absolute energy scale, thus obtaining absolute separation energies; secondly, by keeping the temperature at an optimal value, shell effects are enhanced compared to what they are in vacuum evaporations. The separation energy for a cluster with N atoms is defined as $D(N)=E(N-1)-E(N)$, where $E(N)$ is the total binding energy of cluster size N ($E<0$).

In the present paper we report on clusters evaporating single atoms in an inert gas acting as a heat bath with the temperature regulated by a thermostat. In the experiment we observe the abundance spectrum *after* the clusters reside in the heat bath. In a previous paper [5] we determined the evaporation rate for a few, special Na clusters as a function of the heat bath temperature T; that experiment, together with the present one, are further developments of the preliminary results of Chandezon *et al.* [6].

II. EXPERIMENTS

The experimental setup has been described previously [5,6]. The mass resolution of the time-of-flight spectrometer has been improved to obtain well separated mass peaks in the size range considered, allowing for a precise background subtraction.

Two experiments with nozzles of 1.5- and 1.9-mm diameter are performed. The cluster residence times in the heat bath are 100 ± 20 ms and 60 ± 5 ms, respectively, allowing ample time for several thousand evaporations with subsequent reheating. The He flow velocity in the heat bath and hence the residence time are calculated either from the effective pumping speed or from assuming a Poiseuille flow through the nozzle. The two methods agree quite well, as can be seen from the uncertainties in the residence times, reflecting the deviations in the two methods. As argued previously [5,6], heat conduction by He is very efficient and raising the cluster temperature from the 123 K of the source to that of the thermostat only takes ~3 ms.

The mass spectra have been measured in two series of half a dozen temperatures at the two flow rates. The lowest temperature is room temperature, $T=296$ K, at which no detectable evaporation occurs. At any of the higher temperatures evaporation is observed: a low-temperature range ($T<356$ K) is defined when evaporation is occurring in limited mass regions only, a medium temperature range which is a transitional region, while the high-temperature range ($T>367$ K) is defined when all masses evaporate during the residence time.

The evaporation of one atom leaves the remaining cluster colder by 30–40 K for size $N=140$, i.e., $\sim10\%$ drop in temperature. The subsequent reheating by He collisions is very likely to be fast: at a typical pressure of 5 mbar and $T=323$ K a Na_{140} cluster collides with $\sim5\times10^8$ He atoms per second. This implies that the temperature of the daughter cluster of size $N=140$ comes within 0.4 K of the heat bath temperature in ~10 μs, somewhat faster for lighter clusters. The heat exchange using the molecular-dynamics simulations by Westergren *et al.* [7] is discussed in Appendix A.

III. DATA ANALYSIS

The raw time-of-flight spectra contain an intensity $I_{raw}=I+I_{bkgr}$ in each time slot. The background I_{bkgr} is assumed without shell structure (see Fig. 1). The background seemingly increases with temperature at the position of the most intense peaks, but this is most likely due to resolution defects at the foot of the peaks. After background subtraction the

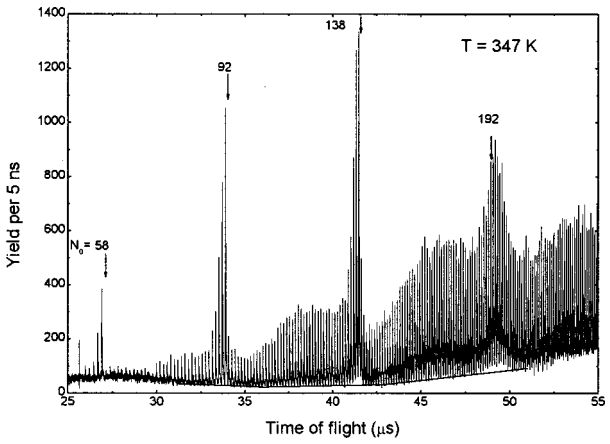

FIG. 1. Untreated time-of-flight spectrum. The closed shells are marked with the number of atoms. A background line is drawn.

distribution is converted to mass units and each peak is integrated to yield $I(N)$. A selection of mass spectra is shown in Figs. 2(a)–2(d). The temperatures quoted are averages of the three thermocouple sensors sitting along the center line of the heat bath; they have uncertainties of ± 3 K.

A. Low temperature

For T being sufficiently low, there is no observable evaporation during the time spent in the heat bath, i.e., the evaporation rate constants, $k(N,T)$, are negligible [Fig. 2(a)]. Raising the temperature in small steps eventually leads to a measurable evaporation of the clusters with the lowest separation energies, i.e., clusters just above a closed electronic shell configuration, N_0 [Fig. 2(b)]. At slightly higher temperature more clusters above N_0 evaporate, leading to an increase of the yield *at* the closed shell. At even more elevated temperatures also clusters at and below the closed shell begin to evaporate [Figs. 2(c) and 2(d)].

In order to obtain decay rates, it is necessary to make some reference to the abundances *prior to* any evaporations. Figure 2(a), properly normalized, represents such a reference. Figure 3 shows the relative yields, where the reference spectrum has been divided out. At moderate temperatures when evaporation only takes place in certain mass regions, where the separation energies are sufficiently low, one may interpolate between regions where no evaporation has taken place. In that process we are guided by the abundance curve taken at room temperature where no shell structure is observed.

The low-temperature range is defined in such a way that evaporation only takes place over a limited range of masses around N_0. In other words, there must be mass regions (with high separation energies) where *no* evaporation occurs. We define higher and lower limits, N_{hi} and N_{lo}, above and below N_0, in such a way that there is only a change of the spectrum inside of these limits, either depletion or accumulation. Initially we interpolate between N_{lo} and N_{hi} to produce a reference curve, i.e., the spectrum prior to any evaporation. A condition here is that the summed amount of missing clusters above N_0, due to evaporations, equals the amount of accumulated clusters at and below N_0. In other words, the integrated area from N_{lo} to N_{hi} between this reference and the spectrum is zero.

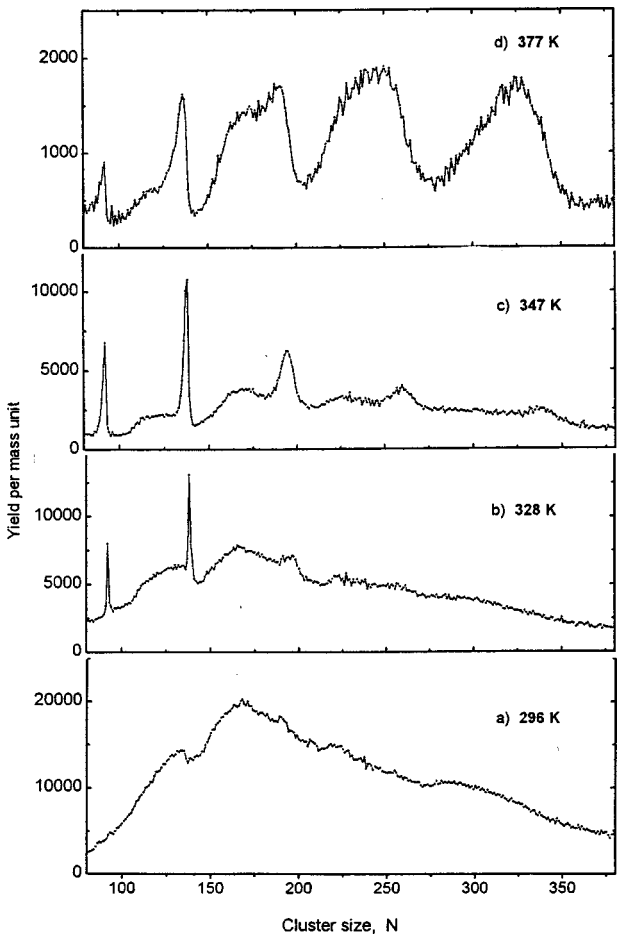

FIG. 2. Mass spectra at four temperatures. (a) 296 K, no observable evaporation. (The reason for the depression around $N \sim 141$ is unknown; it is present at all temperatures and is assumed to have nothing to do with the heat bath, but rather with the formation process itself.) (b) 328 K, only slight evaporation. (c) 347 K, evaporation in certain mass regions only. (d) 377 K, evaporation all over.

The decay constants are found as follows: We begin at $N = N_{\mathrm{hi}}$, descending; for the uppermost cluster size, N_{hi},

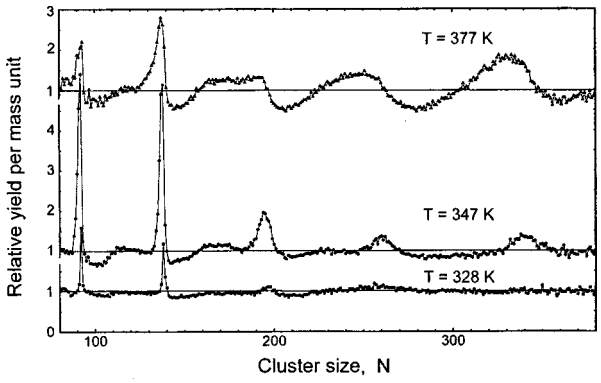

FIG. 3. Spectra of Figs. 2(b)–2(d) normalized to Fig. 2(a), the room-temperature spectrum.

showing deviation between the reference and the original spectrum, one is able to determine a decay constant unambigously. The next lower size, $N_{\rm hi}-1$, has an intensity determined partly by the (now known) decay from $N_{\rm hi}$ above, and partly from the decay to the next one below, $N_{\rm hi}-2$. Thus, the decay constant for $N_{\rm hi}-1$ can be extracted. An analysis like this, down through the chain, ending with $N_{\rm lo}$, allows us to extract decay rates for this limited region.

The method gives a full, systematic determination of absolute decay rate constants in a limited temperature range over larger size regions of clusters. Knowing the residence time of the clusters in the heat bath, the rates convert into (absolute) separation—or dissociation—energies in terms of the Helmholtz free energy. That these values are precisely the separation energy, without any correction from, e.g., the kinetic energy of the evaporated atom, is argued in Appendix B.

This analysis is carried out for temperatures up to and including $T=368$ K and results in an array of decay rates, $k(N,T)$. For each cluster size we are now equipped to produce an Arrhenius plot of $\ln k$ versus $1/T$, see also [5]. However, in order to avoid some of the difficulties associated with this procedure due to the narrow temperature range, we have fixed the preexponential factor independently, making use of vapor pressure tables for sodium [8]. For a recent review on this subject, see [9].

A fit to the vapor pressure is given by the following equation:

$$p_{\rm sat}({\rm Pa}) = 4.752\times 10^9 \exp\left(-\frac{12423.3}{T({\rm K})}\right) = 4.752\times 10^9 \exp\left(-\frac{1.07({\rm eV})}{k_B T}\right). \quad (1)$$

The vapor pressure data used above deal with the enthalpy of evaporation, $H=E+pV$, thus $\Delta H = D'$ with $D' = D+pV$. With the big difference in the densities of condensed and gas phase sodium, the last term can be approximated by $p\Delta V \approx pV = k_B T$ using the ideal gas law for the vapor phase. Introducing this into Eq. (1) is equivalent to renormalizing the prefactor by a factor $1/e$. The bulk dissociation energy fitted from the vapor pressure tables consequently acquires a small energy dependence but is to a good approximation given by the value $D_{\rm bulk}=1.04$ eV in the present temperature interval [11]. The formula (1) then rewrites

$$p_{\rm sat}({\rm Pa}) = 4.752\times 10^9 \exp\left(-\frac{D_{\rm bulk}+k_B T}{k_B T}\right). \quad (2)$$

In the context of the kinetic gas theory, the evaporation rate expresses

$$k = \frac{A}{4}\frac{\bar{v}}{k_B T} p_{\rm sat}, \quad (3)$$

where A is the area of the evaporating surface and $\bar{v} = (8k_B T/m)^{1/2}$ is the mean velocity of the atoms with mass m and $p_{\rm sat}$ the saturated vapor pressure of the solid at the corresponding temperature. We apply expression (3) to clusters using Eq. (2) for $p_{\rm sat}$ and replacing $D_{\rm bulk}$ by the cluster separation energy D. This assumes a similarity between clusters and bulk with respect to the thermal motion of atoms in the surface region. For the spherical cluster surface area we use the expression $A = 4\pi R^2 = 4\pi r_s^2 N^{2/3}$ with the Wigner-Seitz radius $r_s = 2.1$ Å for sodium [10]. We finally get the expression for the evaporation rate of a cluster of size N at temperature T

$$k = \omega \exp\left(-\frac{D+k_B T}{k_B T}\right) = 1.44\times 10^{15}\frac{N^{2/3}}{T^{1/2}}\frac{1}{e}\exp\left(-\frac{D}{k_B T}\right). \quad (4)$$

The formula finally used here is

$$\ln k + \frac{1}{2}\ln T = \ln(1.44\times 10^{15}) + \frac{2}{3}\ln N - 1 - \frac{D}{k_B T}. \quad (5)$$

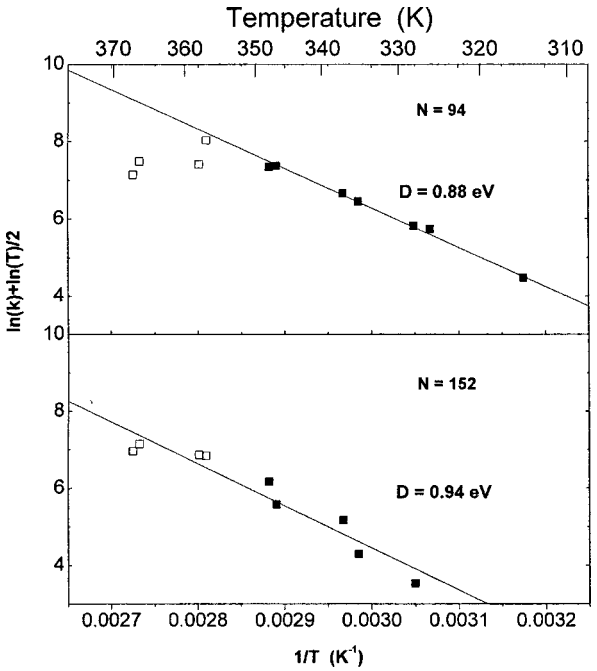

FIG. 4. Arrhenius plots for cluster sizes $N=94$ and 152. Only the filled points are included in the fit. The slope yields a separation energy of $D(94)=0.877\pm 0.001$ eV, with the error reflecting the statistical uncertainty only.

Figure 4 shows two examples of the Arrhenius plots; note that the intercept is determined by the first three terms on the right-hand side of Eq. (4). The general picture is that the points can be fitted with a straight line, albeit some of the points for low masses and higher temperatures deviate, showing a smaller rate than expected from the fit. This effect is discussed in Sec. IV.

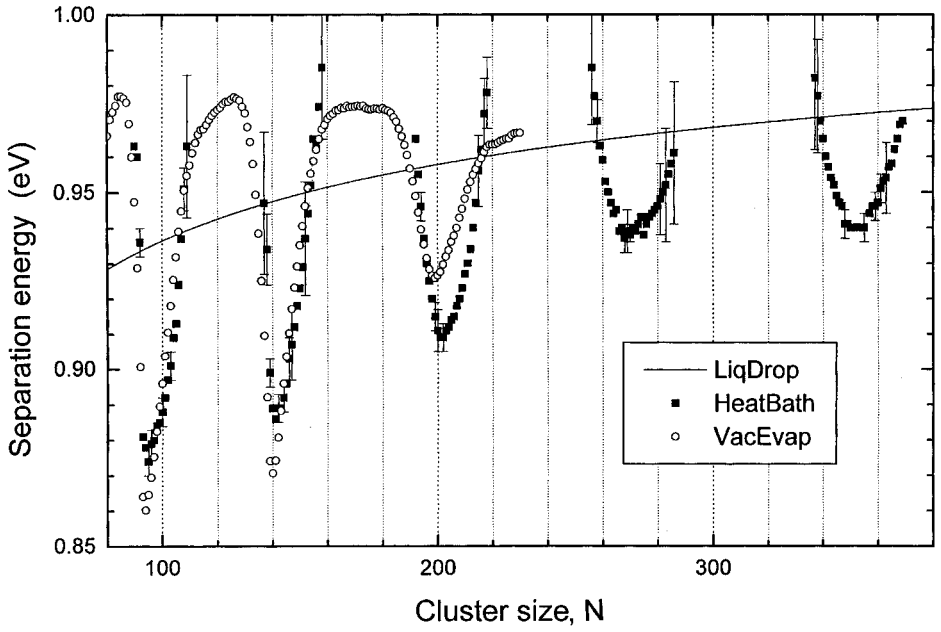

FIG. 5. Separation energies for five mass regions. Filled points: Heat bath measurements. Open points: Vacuum evaporation mesurements [3], normalized to a liquid drop average. Curve: Average liquid drop values [11].

B. High temperature

As seen in Fig. 2(d), at the highest temperatures evaporations are taking place over the whole spectrum, and the procedure used in Sec. III A is not applicable here. On the other hand, simulations over all masses, using previously determined (relative) separation energies [6] show that the flow of evaporations down through the mass chain has *not* reached a steady state. This is confirmed by the observation that the observed abundance pattern varies strongly with temperature. If secular equilibrium had been reached, the abundances would only change due to the small temperature increase involving the Boltzmann factor in a predictable way, and the decrease of shell structure with increasing temperature. None of these effects can, in our opinion, explain the observations and we conclude that a steady-state flow has not yet been reached.

IV. RESULTS AND DISCUSSION

In Fig. 5 are shown the separation energies determined in the five mass regions that could be analyzed with the method described above for the low-temperature data. (The energies are available in tabular form upon request.) The figure also shows the separation energies as determined in vacuum evaporations [3], normalized to the liquid drop separation energies, given by [11]

$$D(N)=a_{\mathrm{V}}-\frac{2}{3}a_{\mathrm{S}}N^{-1/3}, \tag{6}$$

where the two coefficients, the bulk cohesive energy and the surface energy, are equal to 1.04 and 0.72 eV, respectively.

The relative statistical uncertainties in the difference spectra span values between 1% and 6%, averaging around $\pm 4\%$, highest for the low temperatures and for the low-yield regions. We have estimated this by a Monte Carlo simulation by letting the intensities vary in a statistical manner and running the decay chain for each set of intensity values. That procedure also exhibits the strong correlation existing between the individual k values within a decay chain and results in a *relative* uncertainty of only $\pm 0.4\%$. When translated to the ordinate of the Arrhenius plots the results can be seen in Fig. 4. The final uncertainties in the separation energies are indicated in Fig. 5. Concerning the assumption of a structureless background, mentioned in Sec. III, we estimate that the largest error this assumption can result in is ± 0.1 in $\ln k$, which is within the statistical errors, see Fig. 4.

The vacuum evaporation data from previous publications [3] and the heat bath data from the present experiments compare fairly well (see Fig. 5), bearing in mind that the former are relative values, normalized to the liquid drop expression. The heat bath data exhibit a steeper slope at the closed shells, possibly indicating a moderation of the shell energy at the higher temperatures governing the vacuum evaporations [12,13].

Above a certain critical temperature, the measured rates for some cluster sizes diverge significantly from the otherwise fitted straight line in the Arrhenius plots. In the mass region $N=91$–109 this temperature is $T_{\mathrm{crit}}\approx 355$ K. In the region $N=137$–218, $T_{\mathrm{crit}}\approx 360$ K and for $N>256$ we do not observe any deviations, so $T_{\mathrm{crit}}>370$ K. Above T_{crit} we observe a lower rate, as if the actual temperature of the cluster were lower than that of the heat bath. This is not likely to be due to an effect of the clusters not having sufficient reheating time after evaporation; see Appendix A.

There could be two other reasons for the divergence. (1) That the separation energy varies strongly with temperature. This might, for example, be caused by thermally activated shape fluctuations corresponding to a surface roughness, as considered in Ref. [14]. (2) That there is recapture of evaporated atoms by the clusters during their stay in the heat bath. At high temperatures where many atoms are evaporated, the concentration of atoms can be so high that the recapture

probability will significantly alter the abundance spectra. Both of these mechanisms do offer explanations of the deviations in certain mass regions; however, they have to be ruled out because they are at odd with the systematics with respect to N.

The fixed intercept at $1/T=0$ of the Arrhenius curves is determined from bulk data as described in connection with the derivation of Eq. (4). As displayed by the examples in Fig. 4, this value of the intercept is reasonable. In principle, each Arrhenius plot allows for a fit of the data points determining the intercept and the slope independently, that is, both the time scale ω and the separation energy, D. Since the data only cover a narrow interval in inverse temperature, the value of ω will suffer from substantial statistical uncertainty. We find that the Arrhenius plots confirm the value of ω determined from the bulk vapor pressure to roughly a factor of 20 up or down.

Estimates based upon harmonic vibrations in a crystal are found to yield a factor of 10 to 40 faster evaporation than the current value based on saturation pressure data [9]. It would be interesting to see how cluster values for the time scale ω compare to those of the bulk, and whether a deviation could shed light on the atomic motion in the cluster. However, with the present data the uncertainty is too large to address this question.

V. CONCLUSION

It has been demonstrated that it is feasible to perform evaporations from a beam of Na clusters at a well-known and controlled temperature. At several—moderate—temperatures absolute separation energies are extracted and compared to each other in an Arrhenius plot for each cluster mass. A display of ground-state separation energies for extended mass regions between $N=90$ and 370 is produced. The causes for the deviations from the Arrhenius law at higher temperatures are unclear, while several possible reasons are ruled out.

ACKNOWLEDGMENTS

The authors are much obliged to Sven Bjørnholm for his always stimulating and inspiring contributions. They thank Jørgen Schou, Risø National Laboratory for lending his N_2 laser during the initial stages of the experiments. Discussions with Peter Fröbrich and Andrew Jackson are gratefully acknowledged. O.E. wishes to thank the Danish National Bank for accommodation during his sabbatical. The work is supported by the Danish Natural Science Research Council through the research center ACAP with a grant to K.H. and by the European Commission Grant No. CHRX-CT94-0612.

APPENDIX A: HEAT EXCHANGE RATE

The present estimate is based on molecular-dynamics simulations by Westergren *et al.* [7] who use a Lennard-Jones potential for the exchange of energy between the cluster and the inert gas atoms. The average temperature $T_{\mathrm{cl}}(n)$ of a cluster after n collisions with the gas atoms is

$$T_{\mathrm{cl}}(n)=[T_{\mathrm{cl}}(0)-T_{\mathrm{hb}}]\times\left(1-\frac{\kappa}{3Nk_B}\right)^n+T_{\mathrm{hb}}, \quad \text{(A1)}$$

with $T_{\mathrm{cl}}(0)$ as the initial temperature of the cluster just after an evaporation, k_B is the Boltzman constant, and κ is the energy exchange constant for sodium, approximately 31 μeV/K for the relevant temperature range [15]. The fast equilibration means that microscopic thermal equilibrium at the macroscopically measured temperature, T_{hb}, is assured essentially during the entire residence time.

We have looked into the question of the heat contact of clusters with the He atoms. The de Broglie wavelength of the He atoms at thermal energies is approximately 0.5 Å, which is about a factor of four smaller than a typical length scale of the clusters. Also, the thermal energy in the cluster is about a factor of three larger than a typical energy scale, given by the Debye temperature. These two numbers demonstrate that the clusters are not in the limit of small quantum numbers, where we have to apply a quantal calculation. More specifically, they tell that a He atom will be able to exchange momentum in a collision on an individual ion of the cluster, and that there is a sufficient amount of energy states to absorb the momentum delivered. If the de Broglie wavelength had been large compared to the length scale of the cluster, the momentum of the He atom would be transferred coherently to many ions, resulting in an elastic scattering on the cluster as a whole.

These considerations have convinced us in a qualitative way that a classical calculation of the type Westerberg has performed is well justified. It should give a realistic evaluation of the scattering processes themselves and the associated heat exchange.

Reheating and evaporation competes on the time scale where the evaporation rate k_N is comparable to the (inverse) reheating time of the evaporating cluster. For ν being the collision frequency, we define the reheating time τ as the time for the cluster to come within $1/e$ of the final heat bath temperature. Approximated, this is equivalent to $(\tau\nu)\kappa/(3Nk_B)\equiv 1$, where n is substituted by $\nu\tau$ in Eq. (A1). For $\nu=5\times10^8$ s^{-1} this amounts to approximately 1.7 μs or a rate of 6×10^5 s^{-1} for size 100. For rates comparable to or higher than this, one must expect strong corrections to the simple equilibrium rate contants.

In order to get a more precise estimate of the crossover from thermal equilibrium to evaporation limited by insufficient reheating, one can parametrize the problem in terms of an effective cluster temperature T_{cl}, which is ideally equal to the heat bath temperature T_{hb}, but for high rates is lower due to a finite reheating time. This effective temperature is found implicitly by the two coupled equations

$$k_N=\frac{C_v(T_{\mathrm{hb}}-T_{\mathrm{cl}})}{\tau D_N} \quad \text{(A2)}$$

and

$$k_N=\omega\exp(-D_N/k_BT_{\mathrm{cl}}), \quad \text{(A3)}$$

where ω is the (weakly-temperature-dependent) frequency factor given in the main text. Equation (A2) is the stationarity condition for the cluster temperature where the temperature loss rate due to evaporation, $k_N D_N / C_v$, is set equal to the reheating rate $(T_{\rm hb} - T_{\rm cl})/\tau$. These expressions are compared to a Monte Carlo simulation of the evaporation-reheating process and found to agree within 20% even for the highest temperatures in the simulation where the uncorrected heat bath rates $k_{\rm hb}$ exceed the (inverse) reheating time by a factor of 8, i.e., $k_{\rm hb}\tau = 8$. At lower temperatures where the rate is close to the heat bath value, the effective temperature is very close to that of the heat bath and consequently Eq. (A3) can be Taylor expanded from its value at $T_{\rm hb}$ in the small quantity $T_{\rm hb} - T_{\rm cl}$,

$$k_N = \omega \exp(-D_N / k_B T_{\rm hb}) \left(1 + \frac{D_N (T_{\rm hb} - T_{\rm cl})}{k_B T_{\rm hb}^2} + \cdots \right), \tag{A4}$$

and solved with Eq. (A2) to give to first order

$$k_N \approx k_{\rm hb} \left(1 + k_N \frac{D_N^2 \tau}{k_B T_{\rm hb}^2 C_v} \right). \tag{A5}$$

The rate constants are therefore well approximated by the heat bath values provided

$$k_{\rm hb} \frac{D_N^2 \tau}{k_B T_{\rm hb}^2 C_v} \ll 1. \tag{A6}$$

With $D_N / k_B T_{\rm hb} \approx 30$, $\tau = 1.7\, 10^{-6}$ s, and $C_v = 300 k_B$ this gives the limit

$$k_{\rm hb} \ll 2 \times 10^5 ({\rm s}^{-1}) \quad ({\rm for}\ N = 100). \tag{A7}$$

With the scaling $\tau \propto N^{1/3}$ and $C_v \propto N$ this result scales with size as

$$k_{\rm hb} \ll 2 \times 10^5 ({\rm s}^{-1}) \left(\frac{N}{100} \right)^{2/3}. \tag{A8}$$

With the residence time in the heat bath of 0.1 s, this amounts to a relative loss of atoms of

$$\Delta N / N = k_{\rm hb} 0.1({\rm s}) / N \ll 900 N^{-1/3}. \tag{A9}$$

Even for the largest clusters investigated, $N = 400$, this condition is fulfilled since the number corresponds to a loss of more than 125 times of the number of atoms in the cluster. We therefore conclude that the reheating can indeed be considered instantaneous.

APPENDIX B: CORRECTIONS TO THE DISSOCIATION ENERGY

This appendix explains how the slope of the Arrhenius plot is related to the dissociation energy. The question is whether the kinetic energy of the evaporating atom enters into the slope of the Arrhenius plot and similarly whether the thermal excitation energy of the atom in the cluster does. These potential corrections are of magnitude $2k_BT$ and $3k_BT$ and within the precision of the experiment. Furthermore, we discuss the effect of the excitations of the valence electrons in the cluster. These questions can be answered by calculating the rate constants within the detailed balance (Weisskopf) formalism [16]. The rate constants are

$$k_N \propto \int_0^{E - D_N} \epsilon^{1/2} \frac{\rho_1(\epsilon) \rho_{N-1}(E - D_N - \epsilon)}{\rho_N(E)} d\epsilon \tag{B1}$$

for the excitation energy E and the fragment kinetic energy ϵ. Some factors that are immaterial in this connection, mass, etc., are omitted. We can integrate this rate over the equilibrium mother population with the proper canonical ensemble weight given by $[\rho_N(E)/Z_N(T)]\exp(-E/k_BT)$. Then

$$k_N \propto \int_0^{\infty} \int_0^{E - D_N} \epsilon^{1/2} \frac{\rho_1(\epsilon) \rho_{N-1}(E - D_N - \epsilon)}{Z_N(T)} e^{-E/k_B T} d\epsilon\, dE, \tag{B2}$$

where the integral to infinity is the ensemble averaging. Now, ρ_1 is proportional to $\epsilon^{1/2}$. Changing variables from E to $E - D_N - \epsilon$ gives

$$k_N \propto \int_{D_N - \epsilon}^{\infty} \int_0^{E - D_N} \epsilon \frac{\rho_{N-1}(E - D_N - \epsilon)}{Z_N(T)} \times e^{-(E - D_N - \epsilon)/k_B T} e^{-(D_N + \epsilon)/k_B T} d\epsilon\, d(E - D_N - \epsilon). \tag{B3}$$

For all but the very smallest clusters, we can to a good approximation set the upper limit of the integration on the kinetic energy to be infinity. Then we can change the order of integration and perform the mother cluster energy integration first. Integrating over the level density with the Boltzmann factor simply gives the partition function $Z_{N-1}(T)$ of the daughter cluster at temperature T,

$$k_N \propto \frac{Z_{N-1}(T)}{Z_N(T)} \int_{D_N - \epsilon}^{\infty} \epsilon e^{-(D_N + \epsilon)/k_B T} d\epsilon \tag{B4}$$

and then with a last integration

$$k_N \propto \frac{Z_{N-1}(T)}{Z_N(T)} T^2 e^{-D_N / k_B T}. \tag{B5}$$

This result accounts for both the kinetics of the evaporating atom through the factor T^2 and the excitation energy of the atom in the cluster through the ratio of the partition functions Z_{N-1}/Z_N. The phase space of the free atom which gives an average of $2T$ kinetic energy appears as the square of the temperature in the preexponential. The bound atom excitation energy is in a similar way converted to the approximate factor $(\hbar \omega_D / k_B T)^3$ (ω_D is the Debye frequency) which for our purpose is a sufficiently good approximation to the ratio

of the daughter and mother partition functions. Hence the two corrections combine to give a preexponential factor of $(\hbar\omega)^3/k_BT$ and thus do not appear in the exponent.

The electronic excitations play an important role by reducing the magnitude of the shell structure [17]. These excitations can be included by taking the ratio of the ground state electronic partition functions of the two clusters. It gives

$$\frac{Z_{N-1}}{Z_N}=\frac{e^{-F_{N-1}/k_BT}}{e^{-F_N/k_BT}}=e^{-(F_{N-1}-F_N)/k_BT}, \tag{B6}$$

an equation which has been derived previously in a microcanonical context [18]. The free energy is defined having the zero at the electronic ground state of the specific cluster, $F_{N-1}(T=0)=F_N(T=0)=0$.

[1] W.D. Knight, K. Clemenger, W.A. de Heer, W.A. Saunders, M.Y. Chou, and M.L. Cohen, Phys. Rev. Lett. **52**, 2141 (1984).

[2] K. Hansen and U. Näher, Phys. Rev. A **60**, 1240 (1999).

[3] F. Chandezon, S. Bjørnholm, J. Borggreen, and K. Hansen, Phys. Rev. B **55**, 5485 (1997).

[4] S. Bjørnholm and J. Borggreen, Philos. Mag. B **79**, 1321 (1999).

[5] J. Borggreen, F. Chandezon, O. Echt, H. Grimley, K. Hansen, P.M. Hansen, and C. Ristori, Eur. Phys. J. D **9**, 119 (1999).

[6] F. Chandezon, P.M. Hansen, C. Ristori, J. Pedersen, J. Westergaard, and S. Bjørnholm, Chem. Phys. Lett. **277**, 450 (1997).

[7] J. Westergren, H. Grönbeck, S.-G. Kim, and D. Tománek, J. Chem. Phys. **107**, 3071 (1997).

[8] *Handbook of Chemistry and Physics*, edited by R.C. Weast (CRC Press, Cleveland, 1980).

[9] K. Hansen, Philos. Mag. B **79**, 1413 (1999).

[10] N.W. Ashcroft and N.D. Mermin, *Solid State Physics* (CBS Publishing, Philadelphia, 1976).

[11] U. Näher, S. Bjørnholm, S. Frauendorf, F. Garcias, and C. Guet, Phys. Rep. **285**, 245 (1997).

[12] K. Hansen and J. Falk, Z. Phys. D: At., Mol. Clusters **34**, 251 (1995).

[13] P. Brockhaus, K. Wong, K. Hansen, V. Kasperovich, G. Tikhonov, and V.V. Kresin, Phys. Rev. A **59**, 495 (1999).

[14] N. Pavlof and C. Schmit, Phys. Rev. B **58**, 4942 (1998).

[15] J. Westergren (private communication).

[16] V. Weisskopf, Phys. Rev. **32**, 295 (1937).

[17] O. Genzken and M. Brack, Phys. Rev. Lett. **67**, 3286 (1991).

[18] K. Hansen and M. Manninen, J. Chem. Phys. **101**, 10 481 (1994).